Excitation of Superconducting Qubits from Hot Nonequilibrium Quasiparticles

J. Wenner,[1] Yi Yin,[1,*] Erik Lucero,[1,†] R. Barends,[1] Yu Chen,[1] B. Chiaro,[1] J. Kelly,[1] M. Lenander,[1] Matteo Mariantoni,[1,2,‡]
A. Megrant,[1,3] C. Neill,[1] P. J. J. O'Malley,[1] D. Sank,[1] A. Vainsencher,[1] H. Wang,[1,4] T. C. White,[1]
A. N. Cleland,[1,2] and John M. Martinis[1,2,§]

[1]*Department of Physics, University of California, Santa Barbara, California 93106, USA*
[2]*California NanoSystems Institute, University of California, Santa Barbara, California 93106, USA*
[3]*Department of Materials, University of California, Santa Barbara, California 93106, USA*
[4]*Department of Physics, Zhejiang University, Hangzhou 310027, China*
(Received 7 September 2012; revised manuscript received 4 March 2013; published 9 April 2013)

Superconducting qubits probe environmental defects such as nonequilibrium quasiparticles, an important source of decoherence. We show that "hot" nonequilibrium quasiparticles, with energies above the superconducting gap, affect qubits differently from quasiparticles at the gap, implying qubits can probe the dynamic quasiparticle energy distribution. For hot quasiparticles, we predict a non-negligible increase in the qubit excited state probability P_e. By injecting hot quasiparticles into a qubit, we experimentally measure an increase of P_e in semiquantitative agreement with the model and rule out the typically assumed thermal distribution.

Superconducting qubits [1,2] are excellent candidates for building a quantum computer with recent implementations of key quantum algorithms [3,4]. They are also sensitive probes of the physics of microscopic defects which limit coherence such as individual two-level states [5,6], flux noise [7–9], and nonequilibrium quasiparticles [10–16]. The sensitivity of qubits to quasiparticles, and their ability to measure both energy emission and absorption rates, enables new measurements of the nonequilibrium properties of superconductors.

Quasiparticle-induced thermal heating has been attributed as a source [16–19] of qubit excited state populations [16,17,20–24] and excitation rates [18] in excess of thermal equilibrium values. This is supported by the observation that the qubit excited-state population was significantly lowered when the level of stray infrared radiation, and hence quasiparticle density [25], was reduced [16]. In these experiments, the quasiparticle-induced thermal heating necessary to produce the excited state population was thought to result in effective qubit temperatures of 70–200 mK [16–18,20], even though these temperatures are comparable to the qubit energy $E_{ge} \sim 300$ mK. This violates the typical assumptions that $k_B T \ll E_{ge}$ [25,26] or $(E - \Delta) \ll E_{ge}$ [13,26] for characteristic quasiparticle energies E, superconducting gap Δ, and dilution refrigerator temperature $T \simeq 20$ mK. As quasiparticle energies are thus comparable to other relevant energies, the specifics of the quasiparticle energy distribution cannot be neglected.

The quasiparticle energy distribution is frequently taken to be thermal, although sometimes with a quasiparticle temperature distinct from that of the environment [27–31]. This is assumed in single electron transistors [27,28], normal insulator superconductor junctions [30–33], superconducting tunnel junctions [29,34,35], and kinetic inductance

detectors [36,37]. This was even assumed when considering quasiparticle dynamics [28].

Here, we invalidate this assumption using qubit excitation due to quasiparticles, akin to power-generating noise from quasiparticle scattering and recombination in other systems [35–38]. We quantitatively model how high-energy quasiparticles directly excite qubits. We experimentally test this model by injecting a nonequilibrium quasiparticle population into a superconducting qubit and using the qubit to dynamically probe this population. We find semiquantitative agreement between our model and the experimental data presented here, showing that nonequilibrium quasiparticles provide a mechanism for the spurious excitation of superconducting qubits, distinct from thermal effects. We further rule out a thermal distribution for these quasiparticles, even with a distinct quasiparticle temperature. In addition, our approach provides a new method to study the temporal dynamics of the nonequilibrium quasiparticle energy distribution and can be used to validate alternative methods [39].

A quasiparticle tunneling through the Josephson junction barrier in a qubit can cause both excitation and dissipation in the qubit, as illustrated in Fig. 1. Consider a qubit initially in its excited state: a "cold" quasiparticle near the gap energy can absorb the qubit transition energy E_{ge} between the qubit's excited $|e\rangle$ and ground $|g\rangle$ states, causing the qubit to switch to its ground state [blue arrows in Figs. 1(a) and 1(b)]. Any quasiparticle in the junction area can absorb this energy, so the qubit $|e\rangle \rightarrow |g\rangle$ decay rate $\Gamma_\downarrow$ due to this channel is proportional to the quasiparticle density n_{qp}. For a qubit initially in its ground state, a "hot" quasiparticle sufficiently above the gap energy can excite the qubit, but only if the quasiparticle has energy greater than $\Delta + E_{ge}$ [red arrows in Figs. 1(a) and 1(c)].

The qubit $|g\rangle \rightarrow |e\rangle$ excitation rate $\Gamma_\uparrow$ thus depends on the energy distribution of the quasiparticle population.

If the quasiparticle population were well described by a temperature $T \simeq 20$ mK $\ll E_{ge}/k_B$, then a negligible qubit excitation rate $\Gamma_\uparrow$ would be expected, as in Fig. 1(b). There are however a number of processes that can produce quasiparticles with energies well above $k_B T$, which then relax via quasiparticle-phonon scattering [40], but for which the nonequilibrium quasiparticle occupation probability $f(E)$ still has a significant population of hot quasiparticles [11], with energies well above $k_B T$.

In order to model the steady-state quasiparticle distribution, we assume quasiparticles are injected in the junction at a constant rate at an energy E_{inj} well above $\Delta + E_{ge}$, with the resulting quasiparticle density n_{qp} scaling as the square root of the injection rate; we verify below [discussion of Fig. 2(d)] that the qubit excited state probability P_e is independent of the injection energy. Steady state is achieved by balancing phonon scattering and quasiparticle injection and recombination [41]. Although the resulting steady-state occupation probability $f(E)$ has a similar dependence on quasiparticle energy as a 70 mK thermal distribution for $\Delta < E < 1.4\Delta$ [42], no effective temperature can fully describe $f(E)$ for all energies, implying a nonthermal distribution.

With $f(E)$ determined in this manner, we calculate the qubit excitation rate $\Gamma_\uparrow$ and decay rate $\Gamma_\downarrow$. For a tunnel junction with resistance R_T and capacitance C, and for a normalized quasiparticle density of states $\rho(E) = E/\sqrt{E^2 - \Delta^2}$, the qubit decay (excitation) rate induced by all quasiparticles is [11,12]

$$\Gamma_{\downarrow(\uparrow)} = \frac{1 + \cos\phi}{R_T C} \int_{\Delta(+E_{ge})}^{\infty} \frac{dE}{E_{ge}} \frac{E E_f + \Delta^2}{E E_f} \rho(E) \rho(E_f) f(E),$$

(1)

where the final quasiparticle energy $E_f = E + E_{ge}$ ($E_f = E - E_{ge}$) is higher (lower) than E due to the absorption (emission) of the qubit energy E_{ge}. Here, ϕ is the junction phase, which is typically $\phi \simeq 0$ for the transmon and $\phi \simeq \pi/2$ for the phase qubit. For cold nonequilibrium quasiparticles, corresponding to $f(E)$ having population only at the gap energy Δ, this integral gives

$$\Gamma_\downarrow^c = \frac{1 + \cos\phi}{\sqrt{2} R_T C} \left(\frac{\Delta}{E_{ge}}\right)^{3/2} \frac{n_{\text{qp}}}{n_{\text{cp}}}.$$

(2)

Here, $n_{\text{cp}} = D(E_F)\Delta$ is the Cooper pair density, $n_{\text{qp}} = 2D(E_F) \int_\Delta^\infty \rho(E) f(E) dE$ is the quasiparticle density, incorporating both hot and cold quasiparticles, and $D(E_F)/2$ is the single spin density of states. This is the standard result
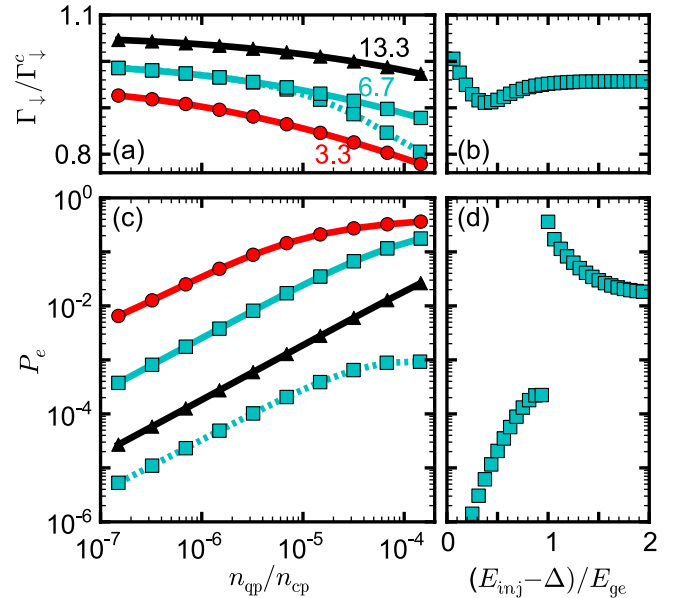
FIG. 2 (color online). Calculated effects of hot quasiparticles. Plots are for three qubit frequencies E_{ge}/h: 13.3 GHz (black), 6.7 GHz (cyan), and 3.3 GHz (red); lines are guides to the eye. Quasiparticle densities incorporate scattering and recombination. (a), (c) Quasiparticles injected at energy $E_{\text{inj}} = 1.8\Delta$ (solid lines) or $\Delta + 0.94E_{ge}$ (dashed line, 6.7 GHz), assuming $\Delta/k_B = 2$ K as for aluminum. (b), (d) Quasiparticle density is $n_{\text{qp}}/n_{\text{cp}} = 10^{-5}$. (a), (b) Qubit decay rate $\Gamma_\downarrow$ normalized by the cold rate $\Gamma_\downarrow^c$ from Eq. (2), showing that $\Gamma_\downarrow^c$ is a good approximation to $\Gamma_\downarrow$. (c) Qubit $|e\rangle$ state probability $P_e = \Gamma_\uparrow/(\Gamma_\downarrow + \Gamma_\uparrow)$ vs normalized quasiparticle density $n_{\text{qp}}/n_{\text{cp}}$. The $|e\rangle$ state occupation increases linearly with the quasiparticle density for low densities. (d) Qubit probability P_e vs injection energy E_{inj} expressed as fraction of E_{ge} above Δ. Injecting low energy quasiparticles results in a greatly reduced P_e. For $E_{\text{inj}} \gtrsim \Delta + 1.7E_{ge}$, P_e is essentially constant.
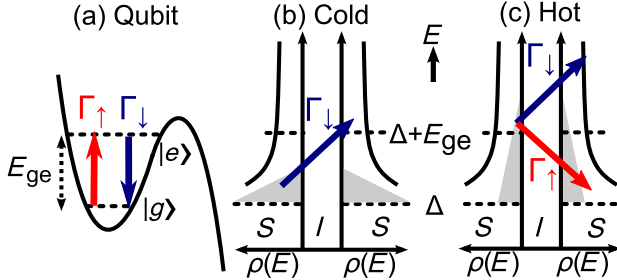

FIG. 1 (color online). Qubit decay $\Gamma_\downarrow$ (blue) and excitation $\Gamma_\uparrow$ (red) mediated by tunneling quasiparticles. (a) Portion of the superconducting phase qubit potential energy diagram, showing the $\Gamma_\downarrow$ and $\Gamma_\uparrow$ transitions between the ground state $|g\rangle$ and the excited state $|e\rangle$, along with the qubit energy E_{ge}. (b) Cold nonequilibrium quasiparticles, which have energies near the superconducting gap Δ, can only absorb E_{ge}, resulting in qubit $\Gamma_\downarrow$ decay. The density of states [$\rho(E)$, horizontal] on both sides of a Josephson junction (superconductor S-insulator I-superconductor S) is shown versus quasiparticle energy E (vertical). The quasiparticle energy distribution $f(E)$ is shown by the shaded triangles. (c) Hot nonequilibrium quasiparticles with energy above $\Delta + E_{ge}$ [portion of $f(E)$ with $E > \Delta + E_{ge}$] not only can cause qubit $\Gamma_\downarrow$ transitions, but can also relax by causing qubit $|g\rangle \rightarrow |e\rangle$ transitions.

for quasiparticle dissipation [13], and is equivalent [12] to the Mattis-Bardeen theory [43] for $\phi = 0$.

In Figs. 2(a) and 2(b) we plot $\Gamma_\downarrow/\Gamma_\downarrow^c$, the ratio of the numerically integrated qubit decay rate $\Gamma_\downarrow$ assuming both hot and cold nonequilibrium quasiparticles [Eq. (1)] to the rate $\Gamma_\downarrow^c$ for cold quasiparticles at the gap [Eq. (2)], with $f(E)$ calculated as explained above. We see that $\Gamma_\downarrow \approx \Gamma_\downarrow^c$ for a range of parameters, so the quasiparticle-induced decay rate is determined primarily by the total quasiparticle density n_{qp} and depends only weakly on the quasiparticle occupation distribution.

However, the quasiparticle distribution is key to characterizing the quasiparticle-induced steady-state excited state population, $P_e = \Gamma_\uparrow/(\Gamma_\downarrow + \Gamma_\uparrow)$. Using the same $f(E)$ as before, we calculate the probabilities plotted in Fig. 2(c). Notice that a non-negligible probability of a few percent can be obtained for quite modest quasiparticle densities. The probability P_e decreases for smaller quasiparticle densities and for larger qubit energies, as expected. For small occupation probabilities, this result can be approximated by the fit function $P_e \simeq 2.17(n_{qp}/n_{cp})(\Delta/E_{ge})^{3.65}$.

To determine the sensitivity of this result to the quasiparticle injection energy, we also calculated P_e as a function of the injection energy E_{inj}. As shown in Fig. 2(d), P_e is independent of the injection energy for $E_{inj} \gtrsim \Delta + 1.7E_{ge}$; hence, for sufficiently large injection energies, the actual injection value is unimportant. In addition, we see that P_e is significantly suppressed for quasiparticle energies below $\Delta + E_{ge}$, demonstrating that cold quasiparticles do not excite the qubit. The maximum at $E_{inj} = \Delta + E_{ge}$ is caused by the peaked final state density of states $\rho(E_f)$ at $E_f = \Delta$ in the expression for $\Gamma_\uparrow$.

To experimentally test these concepts, we performed an experiment in which we deliberately injected quasiparticles into a phase qubit [Figs. 3(a) and 3(b)] and measured the excited state probability P_e and the increase in the qubit decay rate $\delta\Gamma_\downarrow$, which is proportional to n_{qp}/n_{cp} [Eq. (2)]. As shown in Fig. 3(c), we generated quasiparticles by applying a voltage pulse above the gap voltage Δ/e to the qubit's readout superconducting quantum interference device (SQUID). The duration t_{inj} of this pulse was varied to adjust the quasiparticle density and $f(E)$. We reset the qubit into the $|g\rangle$ state using Φ_{bias} and then waited a variable time t_{dif} following the pulse, giving the quasiparticles time to diffuse to the qubit and allowing study of the temporal dynamics. After the qubit control pulses, we measured the qubit P_e, reading out the qubit by increasing V_{sq} to approximately $0.7\Delta/e$ to switch the SQUID into the normal state while minimizing quasiparticle generation. Note this is similar to previous work [12], except here the qubit measurements include the enhancement δP_e versus the energy relaxation rate increase $\delta\Gamma_\downarrow$. The increases δP_e and $\delta\Gamma_\downarrow$, as shown in Fig. 4, are measured by comparing P_e and $\Gamma_\downarrow$ both with and without the quasiparticle injection pulse.
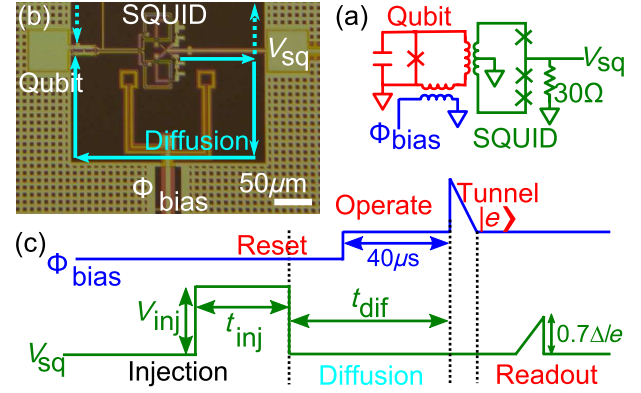

FIG. 3 (color online). Experimental apparatus and protocol. (a) Schematic of phase qubit, with voltage V_{sq} applied to readout SQUID and flux bias Φ_{bias}. Quasiparticles generated with the SQUID can only reach the qubit through the common ground. (b) Photo of qubit. Two paths for quasiparticles to diffuse to the qubit junction are indicated by dotted and solid arrows. (c) Pulse sequence. Quasiparticles are generated with a voltage pulse on the SQUID line of amplitude $V_{inj} > 2(\Delta + E_{ge})/e$ and time t_{inj}, which are varied to adjust the quasiparticle density. After a delay time t_{dif}, 40 μs of which is at the operating bias, allowing quasiparticles to diffuse to the qubit, the qubit state is projected with a flux bias pulse and read out using a voltage pulse on the SQUID.

In Fig. 5, we plot the observed changes δP_e versus $\delta\Gamma_\downarrow$ for two different phase qubits (details in Refs. [4,44], parameters in the Supplemental Material [45]) as we varied t_{dif} and t_{inj} (Fig. 4). We find that δP_e monotonically increases with $\delta\Gamma_\downarrow$, thus scaling with quasiparticle density, as predicted by the theory. As $\delta\Gamma_\downarrow \neq 0$, the quasiparticles
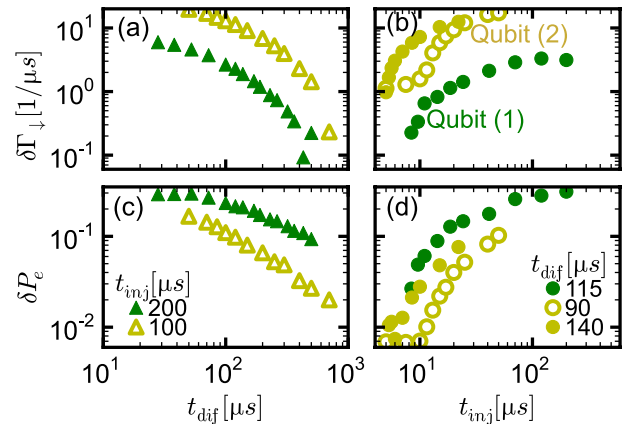

FIG. 4 (color online). Experimental impacts of injected quasiparticles. Increases in (a), (b) qubit decay rate $\delta\Gamma_\downarrow$ and (c), (d) qubit excited state probability δP_e are measured with respect to values without quasiparticle injection. The quasiparticle density was varied by changing (b), (d) the length t_{inj} of the injection pulse or (a), (c) the diffusion time t_{dif}. Data are for two slightly different designs: 1 (Ref. [4]) and 2 (Ref. [44]); experimental parameters are in the Supplemental Material [45]. These increases directly demonstrate a nonequilibrium distribution.

are in a nonequilibrium distribution. In addition, we were able to increase P_e by more than 10%, demonstrating the presence of hot quasiparticles and directly showing that hot quasiparticles can significantly excite the qubit.

The quasiparticle density was changed in three ways: varying the diffusion time t_{dif} (triangles), the injection time t_{inj}, and the injection voltage V_{inj} (open vs closed). There is essentially no difference between changing the injection voltage and the injection time; this makes sense, as P_e is relatively insensitive to the injection energy [Fig. 2(d)]. In addition, for times less than $t_{inj} + t_{dif} \le 350~\mu$s (equality denoted by arrows), the data where t_{dif} was varied are similar to the data where t_{inj} is varied. However, we observed a significant difference with varying the diffusion time for $t_{inj} + t_{dif} > 350~\mu$s. This is not surprising, as P_e is sensitive to the quasiparticle energy distribution, which changes with the diffusion time. As shown in Fig. 3(b), quasiparticles generated at the measurement SQUID must diffuse through approximately $700~\mu$m of ground plane metal in order to reach the qubit junction. This gives time for quasiparticle scattering and relaxation with respect to the injected distribution. In fact, this transition time is consistent with typical quasiparticle recombination times [38,46], where $f(E)$ is expected to become dominated by thermal equilibrium excitation independent of quasiparticle density.

We also considered a thermal quasiparticle distribution, where the quasiparticle temperature was set to give the appropriate $\delta\Gamma_\downarrow$ (dashed line). The only experimental data fit by the thermal model is when t_{dif} is varied for qubit (1), consistent with much of these data having $t_{inj} + t_{dif}$ longer than typical quasiparticle recombination times. For qubit (2), or when t_{inj} is varied, this thermal model does not fit the experimental data in magnitude or slope, indicating a nonthermal distribution.

Predictions from the model are plotted in Fig. 5 as solid lines. Although the power-law dependence (slopes) between model and measurement are in reasonable agreement, the model δP_e is low by about a factor of three for qubit (1) and high by about a factor of four for qubit (2). This can not be attributed to the small differences in the qubit geometries, because a third device (not shown), with the same design as (1), gave data about a factor of two lower than the model. These differences could be due to subtleties in the model not considered here. For instance, there can be sample-to-sample variation such as a difference in film thickness or film quality, yielding variations in the gap energy, in the quasiparticle diffusion path, and in junction parameters. In addition, we note that the calculation of P_e assumes nonequilibrium quasiparticle relaxation through electron-phonon scattering and recombination. Other effects such as quasiparticle diffusion and trapping of quasiparticles from nonuniform gaps may significantly affect the distribution $f(E)$, altering the prediction for the excitation rate; however, such effects are difficult to model due to the qubit geometry [12]. We further assume a constant quasiparticle
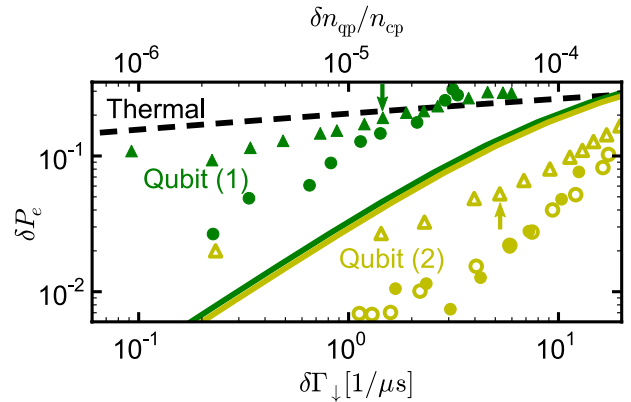

FIG. 5 (color online). Comparison of data and model. The experimental increase in qubit excited state probability δP_e from Fig. 4 is parametrically plotted vs increases in qubit decay rate $\delta\Gamma_\downarrow$, equivalent to the quasiparticle density $\delta n_{qp}/n_{cp}$. Symbols are as in Fig. 4. The power law dependence of δP_e on $\delta\Gamma_\downarrow$ is reduced to the left of $t_{inj} + t_{dif} \sim 350~\mu$s (arrows). Theoretical predictions (solid lines) are for quasiparticles injected at 1.9Δ using measured $E_{ge} \simeq 0.15\Delta$. Dashed line is for a Fermi-Dirac quasiparticle distribution at quasiparticle temperatures selected for $\delta\Gamma_\downarrow$.

injection rate; while this describes infrared-generated quasiparticles, here it may mask effects of the repetition rate and quasiparticle-induced heating. In addition, even though quasiparticles are expected to be generated with energies of $eV_{inj}/2$, in reality, there will be a distribution of quasiparticle energies centered around this value for a given V_{inj}, so even for $eV_{inj} > 2(\Delta + E_{ge})$, some of the generated quasiparticles may instead be cold. We conclude that the simple theoretical model used here for the quasiparticle energy distribution $f(E)$ is only semiquantitative, predicting $\Gamma_\uparrow$ in the nonthermal regime to about a factor of 4.

In conclusion, we have shown that hot quasiparticles with energies greater than $\Delta + E_{ge}$ can cause significant ground-to-excited state transitions in superconducting qubits. This is in contrast to cold quasiparticles solely at the gap, which only cause superconducting qubits to relax. This means quasiparticles cannot be adequately described by a single parameter such as n_{qp}/n_{cp} or temperature. As illustrated by varying both t_{inj} and t_{dif}, the particular quasiparticle distribution affects the observed qubit excitation probability. This theory semiquantitatively matches the observed behavior of the qubit excitation probability versus quasiparticle density, indicating one must consider a nonthermal quasiparticle distribution.

*Present address: Department of Physics, Zhejiang University, Hangzhou 310027, China.

†Present address: IBM T. J. Watson Research Center, Yorktown Heights, NY 10598, USA.

‡Present address: Institute for Quantum Computing and Department of Physics and Astronomy, University of Waterloo, Waterloo, Ontario, Canada N2L 3G1.

§martinis@physics.ucsb.edu

[1] J. Clarke and F. Wilhelm, Nature (London) **453,** 1031 (2008).

[2] J.-S. Tsai, Proc. Jpn. Acad., Ser. B **86,** 275 (2010).

[3] M. D. Reed, L. DiCarlo, S. E. Nigg, L. Sun, L. Frunzio, S. M. Girvin, and R. J. Schoelkopf, Nature (London) **482,** 382 (2012).

[4] E. Lucero et al., Nat. Phys. **8,** 719 (2012).

[5] J. Lisenfeld, C. Müller, J. H. Cole, P. Bushev, A. Lukashenko, A. Shnirman, and A. V. Ustinov, Phys. Rev. Lett. **105,** 230504 (2010).

[6] Y. Shalibo, Y. Rofe, D. Shwa, F. Zeides, M. Neeley, J. M. Martinis, and N. Katz, Phys. Rev. Lett. **105,** 177001 (2010).

[7] S. Gustavsson, J. Bylander, F. Yan, W. D. Oliver, F. Yoshihara, and Y. Nakamura, Phys. Rev. B **84,** 014525 (2011).

[8] D. Sank et al., Phys. Rev. Lett. **109,** 067001 (2012).

[9] S. K. Choi, D.-H. Lee, S. G. Louie, and J. Clarke, Phys. Rev. Lett. **103,** 197001 (2009).

[10] G. Catelani, S. E. Nigg, S. M. Girvin, R. J. Schoelkopf, and L. I. Glazman, Phys. Rev. B **86,** 184514 (2012).

[11] J. M. Martinis, M. Ansmann, and J. Aumentado, Phys. Rev. Lett. **103,** 097002 (2009).

[12] M. Lenander et al., Phys. Rev. B **84,** 024501 (2011).

[13] G. Catelani, J. Koch, L. Frunzio, R. J. Schoelkopf, M. H. Devoret, and L. I. Glazman, Phys. Rev. Lett. **106,** 077002 (2011).

[14] G. Catelani, R. J. Schoelkopf, M. H. Devoret, and L. I. Glazman, Phys. Rev. B **84,** 064517 (2011).

[15] L. Sun et al., Phys. Rev. Lett. **108,** 230509 (2012).

[16] A. D. Córcoles, J. M. Chow, J. M. Gambetta, C. Rigetti, J. R. Rozen, G. A. Keefe, M. B. Rothwell, M. B. Ketchen, and M. Steffen, Appl. Phys. Lett. **99,** 181906 (2011).

[17] K. Geerlings, S. Shankar, Z. Leghtas, M. Mirrahimi, L. Frunzio, R. J. Schoelkopf, and M. H. Devoret, Bull. Am. Phys. Soc. **57,** 1 (2012).

[18] J. E. Johnson, C. Macklin, D. H. Slichter, R. Vijay, E. B. Weingarten, J. Clarke, and I. Siddiqi, Phys. Rev. Lett. **109,** 050506 (2012).

[19] A. Palacios-Laloy, F. Mallet, F. Nguyen, F. Ong, P. Bertet, D. Vion, and D. Esteve, Phys. Scr. **T137,** 014015 (2009).

[20] D. Ristè, C. C. Bultink, K. W. Lehnert, and L. DiCarlo, Phys. Rev. Lett. **109,** 240502 (2012).

[21] M. D. Reed, L. DiCarlo, B. R. Johnson, L. Sun, D. I. Schuster, L. Frunzio, and R. J. Schoelkopf, Phys. Rev. Lett. **105,** 173601 (2010).

[22] R. Vijay, D. H. Slichter, and I. Siddiqi, Phys. Rev. Lett. **106,** 110502 (2011).

[23] K. W. Murch, U. Vool, D. Zhou, S. J. Weber, S. M. Girvin, and I. Siddiqi, Phys. Rev. Lett. **109,** 183602 (2012).

[24] F. Mallet, F. R. Ong, A. Palacios-Laloy, F. Nguyen, P. Bertet, D. Vion, and D. Esteve, Nat. Phys. **5,** 791 (2009).

[25] R. Barends et al., Appl. Phys. Lett. **99,** 113507 (2011).

[26] H. Paik et al., Phys. Rev. Lett. **107,** 240501 (2011).

[27] O.-P. Saira, A. Kemppinen, V. F. Maisi, and J. P. Pekola, Phys. Rev. B **85,** 012504 (2012).

[28] H. S. Knowles, V. F. Maisi, and J. P. Pekola, Appl. Phys. Lett. **100,** 262601 (2012).

[29] F. Giazotto and J. P. Pekola, J. Appl. Phys. **97,** 023908 (2005).

[30] P. A. Fisher, Ph.D. thesis, Harvard University, 1999.

[31] J. P. Pekola, D. V. Anghel, T. I. Suppula, J. K. Suoknuuti, A. J. Manninen, and M. Manninen, Appl. Phys. Lett. **76,** 2782 (2000).

[32] G. C. O'Neil, P. J. Lowell, J. M. Underwood, and J. N. Ullom, Phys. Rev. B **85,** 134504 (2012).

[33] S. Chaudhuri and I. J. Maasilta, Phys. Rev. B **85,** 014519 (2012).

[34] D. R. Heslinga and T. M. Klapwijk, Phys. Rev. B **47,** 5157 (1993).

[35] C. M. Wilson, L. Frunzio, and D. E. Prober, Phys. Rev. Lett. **87,** 067004 (2001).

[36] P. J. de Visser, J. J. A. Baselmans, P. Diener, S. J. C. Yates, A. Endo, and T. M. Klapwijk, Phys. Rev. Lett. **106,** 167004 (2011).

[37] P. J. de Visser, J. J. A. Baselmans, S. J. C. Yates, P. Diener, A. Endo, and T. M. Klapwijk, Appl. Phys. Lett. **100,** 162601 (2012).

[38] R. Barends, J. J. A. Baselmans, S. J. C. Yates, J. R. Gao, J. N. Hovenier, and T. M. Klapwijk, Phys. Rev. Lett. **100,** 257002 (2008).

[39] K. Segall, C. Wilson, L. Li, L. Frunzio, S. Friedrich, M. C. Gaidis, and D. E. Prober, Phys. Rev. B **70,** 214520 (2004).

[40] S. B. Kaplan, C. C. Chi, D. N. Langenberg, J. J. Chang, S. Jafarey, and D. J. Scalapino, Phys. Rev. B **14,** 4854 (1976).

[41] Equations (C3)–(C7) of Ref. [12] are used to calculate the quasiparticle number distribution for a given injection rate. The quasiparticle energy distribution $f(E)$ is then calculated using Eq. (C1), and the total quasiparticle density is calculated with Eq. (C2).

[42] This is determined from the nearly constant slope in the region $1 < E/\Delta < 1.4$ of Fig. 1 in Ref. [11] given $n_{qp}/n_{cp} = 1.8 \times 10^{-6}$ (calculated using Ref. [41]).

[43] D. Mattis and J. Bardeen, Phys. Rev. **111,** 412 (1958).

[44] Y. Yin et al., Phys. Rev. Lett. **110,** 107001 (2013).

[45] See Supplemental Material at http://link.aps.org/supplemental/10.1103/PhysRevLett.110.150502 for experimental parameters and description of device.

[46] B. A. Mazin, D. Sank, S. McHugh, E. A. Lucero, A. Merrill, J. Gao, D. Pappas, D. Moore, and J. Zmuidzinas, Appl. Phys. Lett. **96,** 102504 (2010).